Simulation Experiment on the Influence of Geometric Structure Design of Resonant Tube on Static Stress Distribution and Resonant Frequency

Yilan Xie [1], Yi Yu [2, *]

[1] College of Energy, Xiamen University, Xiamen, China, 361102

[2] School of Energy Science and Engineering, Central South University, Changsha, China, 410083

* Corresponding Author: 8205220514@csu.edu.cn

Abstract. The resonant tube is a key component in thermoacoustic refrigeration machines. Studying the geometric structure of the resonant tube on its static stress distribution, modal and natural frequency can improve the working performance of the resonant tube. This article starts with the working principle and geometric structure design of the resonant tube, then establishes a resonant tube model and analyzes the influence of alternations in the geometric structure parameters of the resonant tube on its static stress distribution and resonant frequency. The research results indicate that the equivalent stress of the mutant resonant tube is the smallest compared to the gradient resonant tube; The resonant frequency of the resonant tube slowly increases with the increase of the opening angle, and rapidly decreases with the increase of the tail cavity radius. Based on the conclusions above, this article explores a method for designing a resonant tube with a specific resonant frequency: by adjusting the geometric parameters of the resonant tube, its resonant frequency will continuously alter and gradually approach the acoustic driving frequency to achieve resonance and output the maximum acoustic pressure. This design method provides important theoretical basis for the design of resonant tubes in practical engineering applications.

Keywords: Resonant tube, Structural design, Static stress analysis, Modal analysis.

1. Introduction

Thermoacoustic refrigeration technology is a new refrigeration technology proposed in the 1980s. Resonant tubes are widely used in thermoacoustic refrigeration machines. The principle of a resonant tube is to use geometric design to reflect and superimpose sound waves inside the tube, forming standing waves or traveling waves, thereby amplifying sound pressure oscillations and maintaining the required sound field of the system. In a thermoacoustic refrigeration unit, the resonant tube transfers acoustic energy from the sound source to the thermoacoustic stack. By adjusting the sound field distribution, generating and maintaining acoustic oscillations, it drives the thermodynamic cycle of the working fluid and improves refrigeration efficiency. Therefore, studying and optimizing the structural design scheme of resonant tubes to improve their working efficiency is of great practical significance for the development of thermoacoustic refrigeration technology and the improvement of energy utilization efficiency.

In recent years, significant research progress has been made in various aspects of resonant tubes for thermoacoustic refrigerators both domestically and internationally. Yu Yanan et al. [1] found that the total length of the resonant tube determines the approximate range of the resonant frequency, while the ratio of the length to the diameter of the sub tube determines the precise value of the resonant frequency and the relationship between the resonant frequency of each mode. The research team of Xi'an Jiaotong University proposed a new type of gas-liquid coupled double acting traveling wave thermoacoustic refrigeration system. The system structure size was optimized through numerical simulation, and it was found that with the increase of system stages, the power density of the whole machine increased [2]. Hu Anqi et al. [3] found that the small gap at the closed end of the acoustic resonant tube can change its resonant frequency. The frequency increases with the increase of the hole area, and the growth rate is first fast and then slow.

The research on resonant tubes in thermoacoustic refrigerators is more mature abroad. Tests were conducted on the temperature differences of resonators with different stacks used in a simple thermoacoustic refrigerator at five different positions, and it was found that the longer stack with the smallest porosity produced the best results at the position closest to the acoustic driver [4]. Sun W et al. [5] revealed the acoustic matching mechanism of the Speaker Driven Thermoacoustic Refrigeration System (LSTAR), and found that the radial size of the system and the electromechanical parameters of the speaker are the key factors determining the matching effect. In terms of nonlinear acoustic and thermodynamic coupling effects, researchers have further revealed the complex mechanism of the interaction between sound waves and heat flow in thermoacoustic tubes through numerical simulations and experimental verification [6].

This article innovatively starts with the geometric structure design of the resonant tube, exploring the influence of the geometric structure of the resonant tube on its working performance. This article uses SolidWorks to establish resonant tube models with different geometric structural parameters, and uses ANSYS simulation software for stress analysis and modal analysis to explore the relationship between the static stress, operating frequency, opening inclination angle, and tail cavity radius of the resonant tube.

2. Theoretical basis for numerical simulation of thermoacoustics

The use of computational fluid dynamics software Solidworks to simulate the acoustic flow field inside the resonant tube of a thermoacoustic refrigeration machine is a process of using numerical methods to solve the partial differential equations that are difficult to solve in thermoacoustic problems, in order to obtain the numerical solution of the required scalar. The theoretical basis involved in this numerical simulation process includes the thermoacoustic theory foundation and the numerical processing foundation of the software itself [7].

2.1. The thermodynamic basis of thermoacoustics

The foundation of thermodynamics is the first and second laws of thermodynamics. Heat can be transferred from one object to another, or converted into mechanical or other energy, but the total value of energy remains constant during the conversion process; The increase in internal energy of an object is equal to the sum of the heat absorbed by the object and the work done on the object. This is the first law of thermodynamics [8]:

$$dU = \delta Q - \delta W \tag{1}$$

Heat cannot spontaneously transfer from low-temperature objects to high-temperature objects. This is the Clausius formulation of the second law of thermodynamics. In natural processes, the entropy of an isolated system does not decrease. That is:

$$dS \geq \delta Q / T \tag{2}$$

2.2. Acoustic Fundamentals of Thermoacoustics

For thermoacoustic resonant tubes, physical parameters such as sound pressure and particle vibration velocity, temperature and density in the acoustic flow field inside the tube are important. Taking compressible simple fluids as the research object, assuming that the sound amplitude is small and the solid medium is rigid and fixed, based on first-order acoustic content and linear N-S equations, energy equations, etc., the following equations expressing physical quantities are obtained [9]:

Sound pressure equation:

$$p = p_m + Re[p_1(x)e^{iwt}] \tag{3}$$

Velocity equation:

$$u = Re[u_1(x, y, z)e^{iwt}] \tag{4}$$

Temperature equation:

$$T = T_m + Re[T_1(x, y, z)e^{iwt}] \tag{5}$$

Density equation:

$$\rho = \rho_m + Re[\rho_1(x, y, z)e^{iwt}] \tag{6}$$

Displacement equation:

$$s = s_m + Re[s_1(x, y, z)e^{iwt}] \tag{7}$$

2.3. Fundamentals of Fluid Mechanics in Thermoacoustics

The foundation of fluid mechanics in thermoacoustic mainly includes three main equations: the conservation of mass equation, the conservation of momentum equation, and the energy equation.

Continuity equation:

$$\frac{\partial \rho}{\partial t} + \nabla(\rho v) = 0 \tag{8}$$

Momentum equation:

$$\rho[\frac{\partial v}{\partial t} + (v \cdot \nabla)v] = -\nabla P + \mu \nabla^2 v \tag{9}$$

Energy equation:

$$\frac{\partial}{\partial t}(\rho\epsilon + \frac{1}{2}\rho|v|^2) = -\nabla \cdot \left[-k\nabla T - v\sigma' + (\rho h + \frac{1}{2}\rho|v|^2)v\right] \tag{10}$$

Combine the three equations to obtain the entropy equation:

$$\rho T(\frac{\partial S}{\partial t} + v \cdot \nabla S) = \nabla \cdot k\nabla T - k\frac{|\nabla T|^2}{T} + \rho T S_{gen}, S_{gen} \geq 0 \tag{11}$$

3. Construction of Resonant Tube Model

The resonant tube is an important component of standing wave thermoacoustic refrigeration machines, which can store some acoustic energy and adjust the resonant frequency. The relevant model parameters can have a significant impact on the refrigeration of the refrigeration machine. The resonant frequency of the heat engine should be close to or consistent with the design frequency. The resonant tube can be divided into two forms: 1/4 wavelength and 1/2 wavelength. At the open end, the pressure reaches its maximum value and the velocity is zero; At the end, the opposite is true, with the minimum pressure and the maximum speed achieved.

The length of a resonant tube in the form of 1/4 wavelength is determined by operating frequency [10]. If L is the length of the resonant tube, c is the speed of sound and f is the design frequency, then:

$$L = \frac{c}{4f} \tag{12}$$

Using 2000 Hz as the design frequency and a sound velocity of 340m/s, according to the above formula, the length of the resonant tube should be designed to be 42.5 mm. Take 40 mm as the length of the resonant tube, with an axial length of 4mm for the front opening, 21 mm for the middle lumen, and 15 mm for the tail lumen. The radius of the middle lumen is taken as 4 mm; The opening angle changes from 30o to 60o, and the diameter of the front opening changes with the change in opening angle; The radius of the tail cavity is taken as 15 mm. The structural design of the resonant tube mentioned above is shown in Figure 1 and 2.

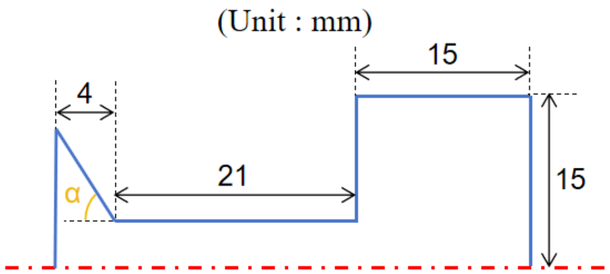

Figure 1. Cross sectional structural diagram of resonant tub

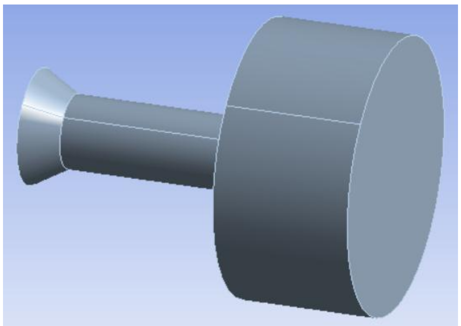

Figure 2. Stereoscopic structural diagram of the resonant tube

4. Equivalent stress analysis of resonant tube model

4.1. Material setting and grid division

The resonant tube is manufactured by structural steel, and its characteristic parameters are shown in Table 1.

Table 1. Characteristic parameters of structural steel used in resonant tubes

Material	Structural steel
thickness d	2mm
density ρ	7850 kg/m^3
Elastic modulus E	2.06×10^{11} Pa
Poisson's ratio μ	0.28

Build a set of thermoacoustic tube models using the software SolidWorks, and gradually increase the inclination angle (α angle in Figure 1) of the left lumen of each model from 30o to 60o to explore the influence of the thermoacoustic tube structure on its static stress distribution and mode.

In software ANSYS Workbench, add the "Static Structure" analysis system, import the established resonant tube structure model into it, set the grid size to 2mm, and establish the grid. The total number of nodes in the obtained grid is 19000-21500, and the number of units is 13000-14000. The generated grid is shown in Figure 3. The left end face of the model is set as a fixed surface, and a static stress of 500N is applied at the junction of the left lumen and the middle lumen, as shown in Figure 4.

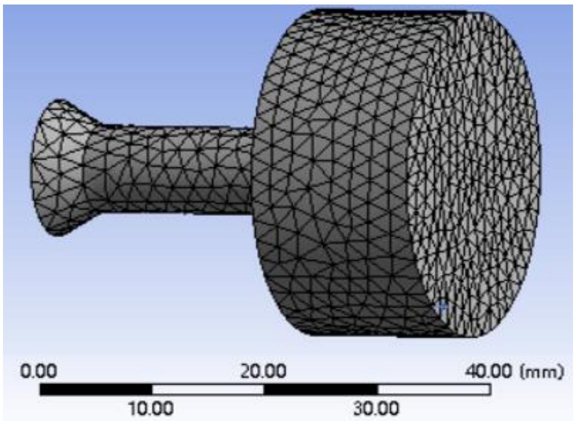

Figure 3. Grid division results

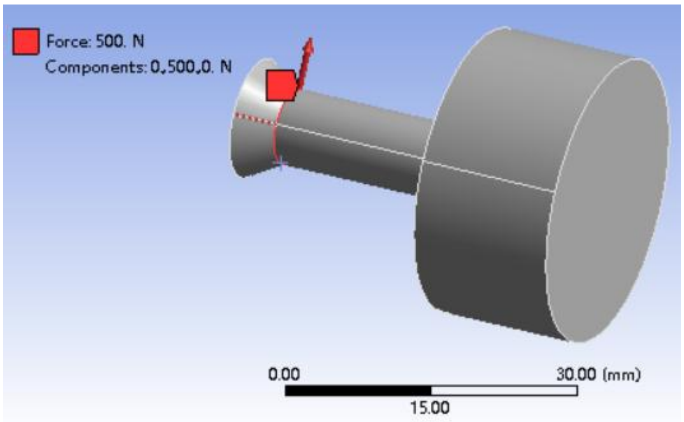

Figure 4. Constraints and Force Settings

Based on the divided grid, the equivalent static stress of the models with different inclination angle are analyzed. The results are shown in Figure 5 to 11.

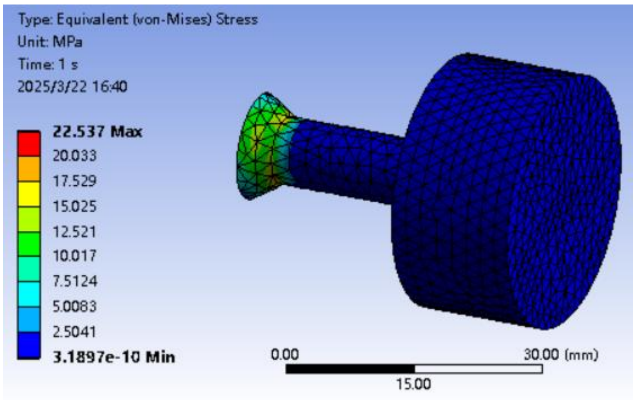

Figure 5. Inclination angle: 30°

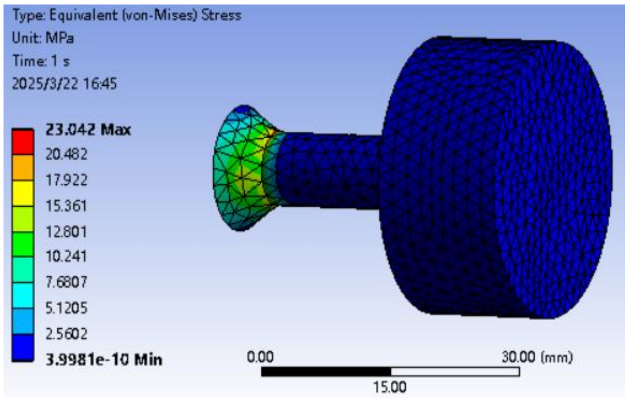

Figure 6. Inclination angle: 35°

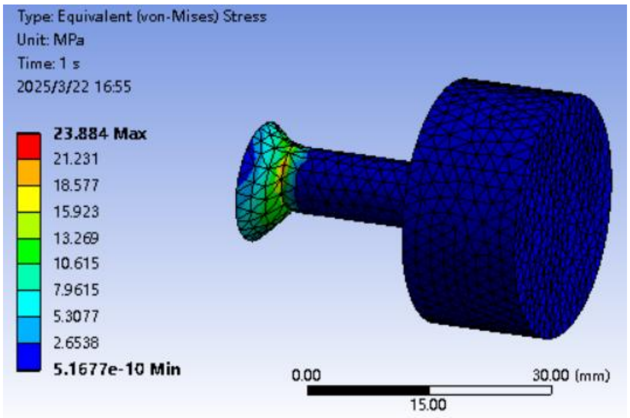

Figure 7. Inclination angle: 40°

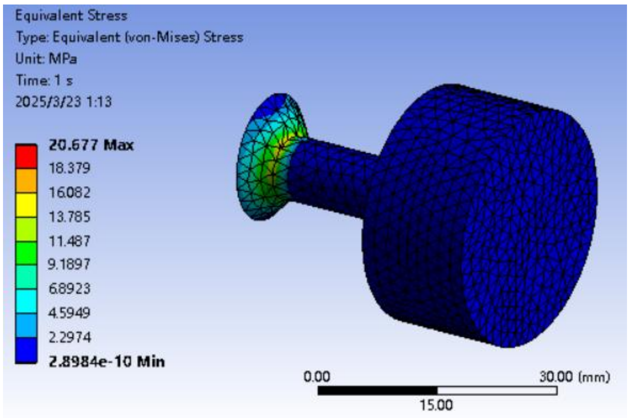

Figure 8. Inclination angle: 45°

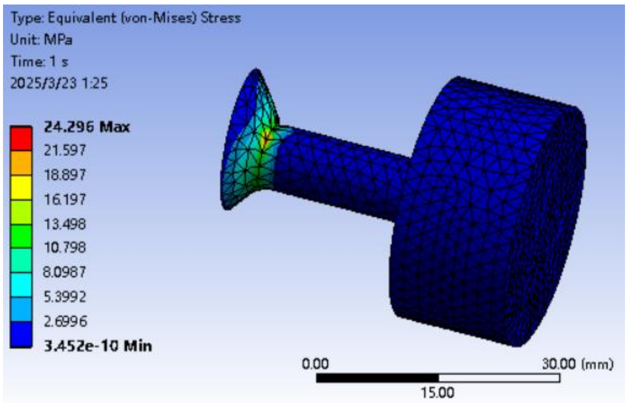

Figure 9. Inclination angle: 50°

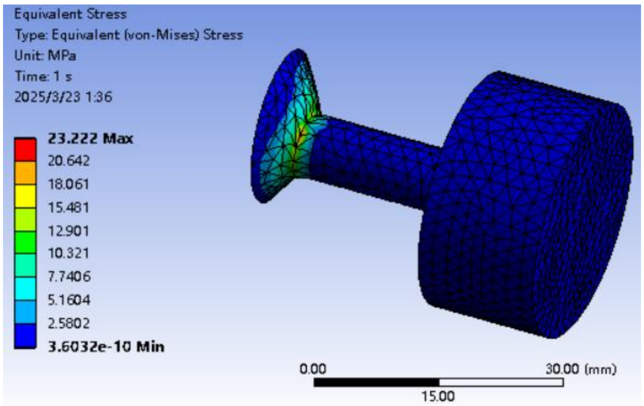

Figure 10. Inclination angle: 55°

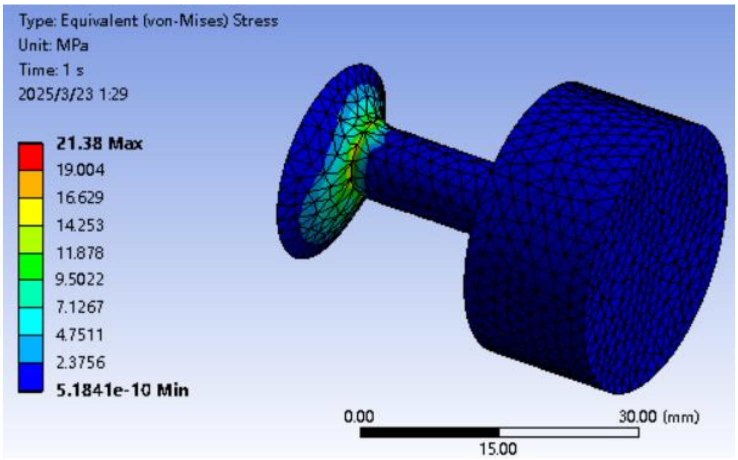

Figure 11. Inclination angle: 60°

Replace the gradient resonant tube with a mutant resonant tube, and its geometric structure is shown in Figure 12. Using the same parameters and methods for static stress analysis, the results are shown in Figure 13.

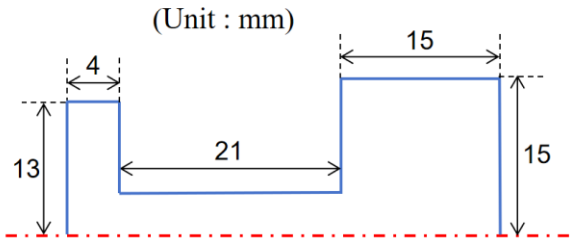

Figure 12. The cross-sectional structure of the mutant resonant tube

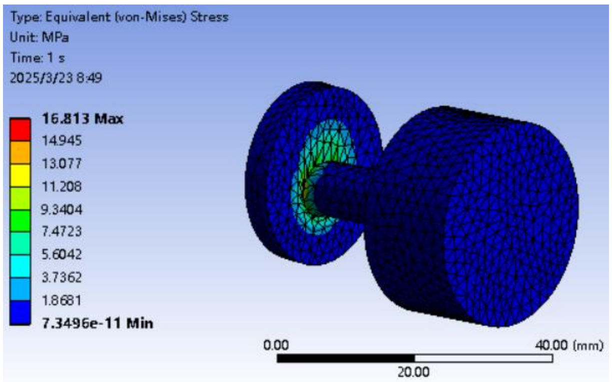

Figure 13. Stress analysis of mutant resonant tube

Draw the above research results into a table, and the equivalent stress extreme values of the resonant tube at each angle are shown in Table 2.

Table 2. Equivalent stress extremum of resonant tubes at various inclination angles

Inclination angle	Maximum equivalent stress / Pa	Minimum equivalent stress /10^{-9} Pa
30°	20.139	3.4459
35°	18.135	3.0117
40°	19.270	1.4275
45°	17.371	4.4166
50°	18.816	7.2021
55°	16.292	1.8778
60°	17.945	4.2661
90°	12.393	3.7058

From the results, we can see that when the inclination angle is 55o, the resonant tube model as a whole experience the minimum equivalent stress, with a maximum equivalent stress of 16.292 Pa. The stress distribution of various resonant tubes follows the following pattern: the equivalent stress is highest on the stress line (the connection circumference between the left and middle lumens), gradually decreases near the connection surface, and relatively lowest on the tube surfaces far from the stress point.

The equivalent stress of the mutant resonant tube at the junction of the two tube sections is significantly lower than that of each gradual resonant tube, with a maximum equivalent stress of 12.393Pa, which is 31.7% lower than that of the gradual resonant tube with an inclination angle of 55o; the minimum equivalent stress is 3.7058×10^{-9} Pa, which is 13.1% lower than the gradient resonant tube with an inclination angle of 55o.

5. Modal analysis of the resonant tube

We model the resonant tube, conduct modal analysis, adjust the cavity size, and gradually approach the design frequency. When the design frequency is basically the same as the driving frequency, resonance occurs, resulting in the highest sound pressure and the strongest sound field, effectively improving the efficiency of the thermoacoustic refrigeration machine.

5.1. Exploring the Influence of Inclination Angle on Resonant Frequency

The material of the resonant tube is structural steel. In ANSYS Workbench software, add a "modal" analysis system and import the established resonant tube structure model into the mechanical module. Set the mesh size to 2mm and create a mesh. The obtained grid has a total of 20000~22000 nodes and 13000~14000 units.

The left end face of the resonant tube is set as a fixed surface constraint, with no constraint force, and the maximum modal order is set to 6. Taking a resonant tube with an opening angle of 30o as an example, the 1st to 6th modes of vibration were calculated, and the results are shown in Figures 14 to 19. From the various modes shown in the Figure, it can be seen that the first and second modes are characterized by shaking changes, the third mode is characterized by radial changes that meet the requirements, and the fourth and fifth modes are characterized by shaking changes. Therefore, the third mode of vibration is what we need.

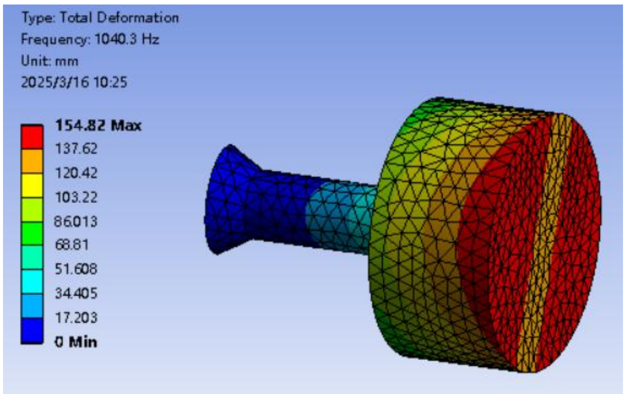

Figure 14. 1st order mode of vibration

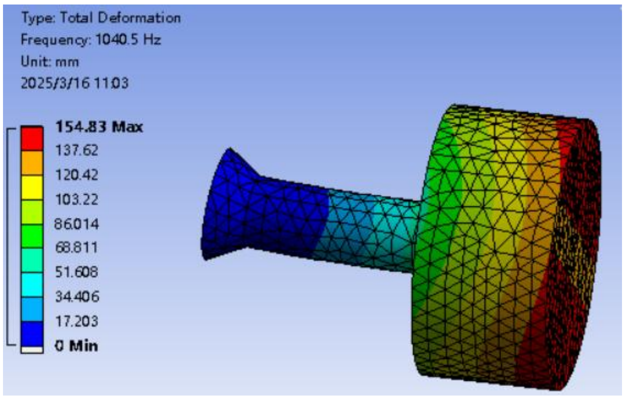

Figure 15. 2nd order mode of vibration

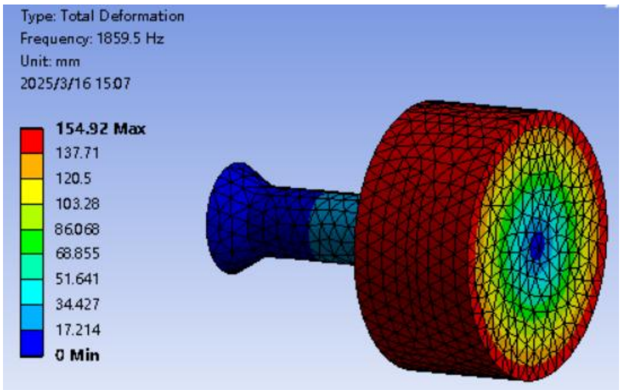

Figure 16. 3rd order mode of vibration

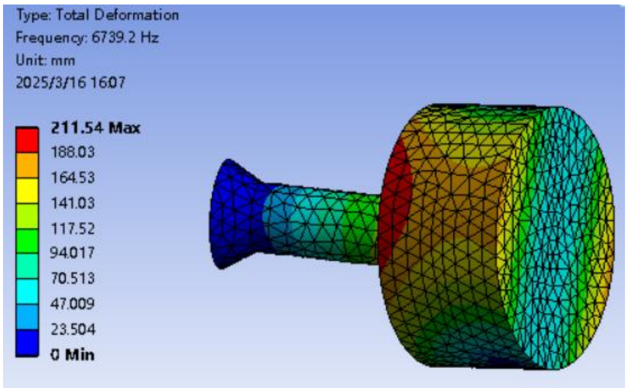

Figure 17. 4rd order mode of vibration

Alter the inclination angle of the resonant tube and explore the effect of the opening angle of the resonant tube on the resonant frequency. The resonant frequencies of each order mode of the resonant tubes are shown in Figure 20 to 27.

	Mode	☑ Frequency [Hz]
1	1.	1040.3
2	2.	1040.5
3	3.	1859.5
4	4.	6739.2
5	5.	6741.6
6	6.	10452

Figure 20. Inclination angle: 30°

	Mode	☑ Frequency [Hz]
1	1.	1046.1
2	2.	1046.3
3	3.	1865.6
4	4.	6778.4
5	5.	6780.8
6	6.	10474

Figure 21. Inclination angle: 35°

	Mode	☑ Frequency [Hz]
1	1.	1053.8
2	2.	1055.5
3	3.	1876.5
4	4.	6869.5
5	5.	6912.6
6	6.	10521

Figure 22. Inclination angle: 40°

	Mode	☑ Frequency [Hz]
1	1.	1054.3
2	2.	1054.6
3	3.	1874.3
4	4.	6822.2
5	5.	6823.6
6	6.	10502

Figure 23. Inclination angle: 45°

	Mode	Frequency [Hz]
1	1.	1057.1
2	2.	1057.6
3	3.	1877.7
4	4.	6840.4
5	5.	6846.5
6	6.	10513

Figure 24. Inclination angle: 50°

	Mode	Frequency [Hz]
1	1.	1059.8
2	2.	1059.9
3	3.	1880.7
4	4.	6854.6
5	5.	6859.5
6	6.	10522

Figure 25. Inclination angle: 55°

	Mode	Frequency [Hz]
1	1.	1060.9
2	2.	1061.4
3	3.	1883.2
4	4.	6860.7
5	5.	6865.4
6	6.	10526

Figure 26. Inclination angle: 60°

	Mode	Frequency [Hz]
1	1.	1065.6
2	2.	1065.8
3	3.	1893.8
4	4.	6893.4
5	5.	6897.5
6	6.	10543

Figure 27. Inclination angle: 90°

According to experimental data, as the opening angle of the resonant tube increases, the resonant frequencies of each mode of the resonant tube slowly increase. When the order is fixed, for every 5o increase in the opening angle of the resonant tube, the resonant frequency increases by an average of 0.3%. When the opening angle of the resonant tube is fixed, the higher the order, the higher the resonant frequency. Among them, the resonant frequencies of the 1st and 2nd, 4th and 5th modes of each resonant tube are very close, and there are significant differences between the 6th resonant frequency, 4th and 5th resonant frequencies, and the 1st, 2nd, and 3rd resonant frequencies.

5.2. Exploring the Influence of the Tail Cavity Radius on the Resonant Frequency

On the basis of exploring the influence of opening angle on its resonant frequency, the tail cavity radius of the resonant tube was changed to investigate the effect of the change in tail cavity radius on the resonant frequency. Build the corresponding resonant tube model in SolidWorks, with the tail cavity radius varying from 15 mm to 22 mm, increasing by 1 mm each time. The remaining geometric parameters are consistent with Figure 1.

Set the grid size to 2 mm and establish a grid. The total number of nodes in the obtained grid is 27000~40000, and the number of elements is 18000~27200 (the larger the tail cavity radius, the more nodes and elements there are). The left end face of the resonant tube is set as a fixed surface constraint, with no constraint force, and the maximum modal order is set to 6. Represented by a resonant tube with an opening angle of 60o, the resonant frequencies of the first to sixth orders of the resonant tube were calculated for different tail cavity radius. The experimental results are shown in Figure 28 to 35.

	Mode	Frequency [Hz]
1	1.	1040.3
2	2.	1040.5
3	3.	1859.5
4	4.	6739.2
5	5.	6741.6
6	6.	10452

Figure 28. Tail Cavity Radius: 15 mm

	Mode	Frequency [Hz]
1	1.	968.51
2	2.	968.62
3	3.	1635.
4	4.	6097.9
5	5.	6100.5
6	6.	9792.4

Figure 29. Tail Cavity Radius: 16 mm

	Mode	Frequency [Hz]
1	1.	905.73
2	2.	906.05
3	3.	1449.4
4	4.	5544.5
5	5.	5550.6
6	6.	9209.7

Figure 30. Tail Cavity Radius: 17 mm

	Mode	Frequency [Hz]
1	1.	847.85
2	2.	847.86
3	3.	1292.1
4	4.	5052.3
5	5.	5054.9
6	6.	8680.

Figure 31. Tail Cavity Radius: 18 mm

	Mode	Frequency [Hz]
1	1.	796.66
2	2.	796.76
3	3.	1159.8
4	4.	4634.8
5	5.	4638.6
6	6.	8211.2

Figure 32. Tail Cavity Radius: 19 mm

	Mode	Frequency [Hz]
1	1.	750.2
2	2.	750.3
3	3.	1046.8
4	4.	4262.1
5	5.	4262.6
6	6.	7782.7

Figure 33. Tail Cavity Radius: 20 mm

	Mode	Frequency [Hz]
1	1.	708.12
2	2.	708.29
3	3.	949.57
4	4.	3939.4
5	5.	3941.3
6	6.	7397.3

Figure 34. Tail Cavity Radius: 21 mm

	Mode	Frequency [Hz]
1	1.	669.47
2	2.	669.5
3	3.	865.09
4	4.	3647.5
5	5.	3650.4
6	6.	7041.6

Figure 35. Tail Cavity Radius: 22 mm

According to experimental data, as the tail cavity radius of the resonant tube increases, the resonant frequencies of each order of the resonant tube will significantly decrease. During the process of changing the tail cavity radius from 15 mm to 22 mm, the 1st and 2nd order resonant frequencies of the resonant tube decreased by 35.6%, the 3rd order decreased by 53.4%, the 4th and 5th order decreased by 45.8%, and the 6th order decreased by 32.6%. The average resonant frequency of each mode was 41.47%; On average, for every 1 mm increase in the tail cavity radius, the resonant frequency decreases by 5.9%.

Under the premise of a change in the tail cavity radius, the law that the higher the order of the resonant tube, the higher the resonant frequency still holds, and the law that the resonant frequencies of the 1st and 2nd, 4th and 5th modes of each resonant tube are very close still holds.

5.3. Design Resonant Tubes with Specific Resonant Frequencies

From the above experimental results, it can be concluded that: the resonant frequency of the resonant tube slowly increases with the increase of the opening angle, and rapidly decreases with the increase of the tail cavity radius. Based on this conclusion, resonant tubes with specific resonant frequencies can be designed by continuously adjusting and optimizing the parameter combination of the opening angle and tail cavity radius of the resonant tube.

As mentioned earlier, this article is designed with a frequency of 2000 Hz. In the second part of the modal analysis experiment, the third-order resonant frequency of the resonant tube with an opening angle of 30o and a tail cavity radius of 15 mm was 1859.5 Hz, which is close to 2000 Hz. Therefore, we adjusted the experimental parameters based on this resonant tube in order to accurately adjust its resonant frequency to 2000 Hz.

Based on the conclusions from the static stress analysis experiment, the opening angle of the resonant tube was set to 90o (i.e., the mutant resonant tube) to make its equivalent stress relatively small. The modal analysis results indicate that the resonant frequency of the third-order mode of the resonant tube with a sudden change and a tail cavity radius of 15 mm is 1893.9Hz, slightly lower than the design frequency of 2000 Hz. Therefore, the tail cavity radius should be further increased. After repeated experimental analysis and comparison, we found that when the tail cavity radius is 14.6 mm, its third-order resonant frequency is 1998.6 Hz, which is extremely close to the design frequency. The geometric structure diagram, static stress analysis, and modal analysis results of this resonant tube (mutant, tail cavity radius 20.8 mm) are shown in Figure 36-39.

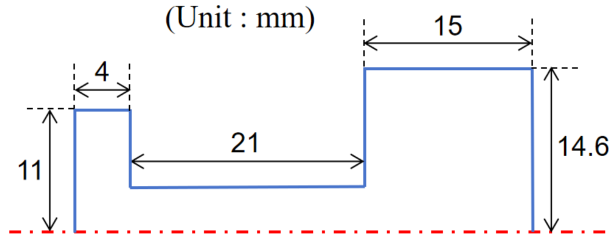

Figure 36. Cross sectional structural diagram of the designed resonant tube

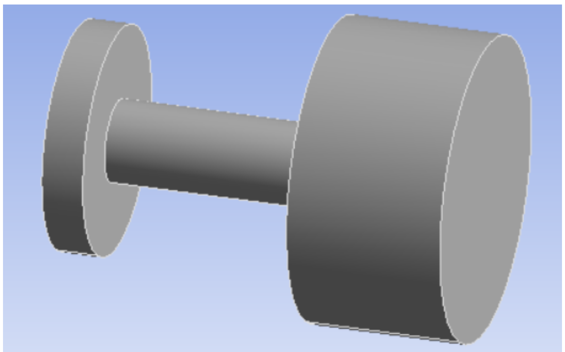

Figure 37. Stereoscopic structural diagram of the designed resonant tube

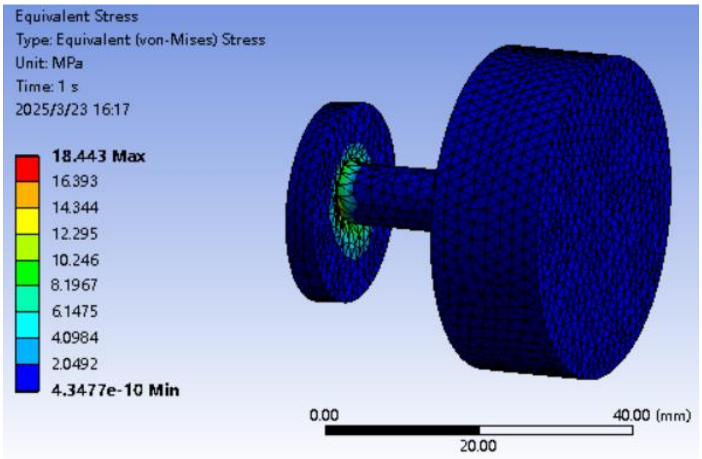

Figure 38. Static stress analysis results

	Mode	✔ Frequency [Hz]
1	1.	1098.
2	2.	1098.1
3	3.	1998.6
4	4.	7182.5
5	5.	7194.7
6	6.	10834

Figure 39. Modal analysis results

5.4. Summary of the Modal Analysis

This chapter establishes resonant tube models with different geometric structures and explores the effects of the opening angle and tail cavity radius of the resonant tube on the resonant frequencies of each order. The simulation experiment results show that the first and second modes of vibration are characterized by shaking changes, the third mode is characterized by radial changes that meet the requirements, and the fourth and fifth modes are characterized by shaking changes; The resonant frequency of the resonant tube slowly increases with the increase of the opening angle, and for every 5o increase, the resonant frequency increases by about 0.3%; The resonant frequency also rapidly decreases with the increase of the tail cavity radius, with a decrease of approximately 5.9% for every 1mm increase in radius.

Based on the above experimental conclusions, we designed the resonant tube with the minimum equivalent static stress as the base plate, continuously changed its tail cavity radius, and comprehensively designed the geometric structure of the resonant tube to achieve the effect of the design frequency being basically consistent with the driving frequency. At this time, the sound pressure is the highest and the working performance is the best. We found that the resonant tube with the cross-sectional structure shown in Figure 36 (as shown in Figure 37) has a resonant frequency of 1998.6 Hz, which is highly close to the operating frequency, under the condition of low equivalent stress, perfectly completing the design of the resonant tube. This chapter innovatively opens up a new method for adjusting the resonant frequency of the resonant tube, which is beneficial for the practical engineering application of the resonant tube design in thermoacoustic refrigeration machines. By continuously adjusting and optimizing the opening angle and tail cavity radius, resonant tubes with other resonant frequencies can also be designed.

6. Conclusion

This article systematically studies the influence of the geometric structure of the resonant tube in a thermoacoustic refrigeration machine on its static stress distribution, mode, and resonant frequency through numerical simulation and experimental analysis. Firstly, resonant tube models with different geometric structures were established using SolidWorks and static stress analysis and modal analysis were conducted using ANSYS software. The research results indicate that geometric parameters such as the opening angle, tail cavity length, and tail cavity radius of the resonant tube have a significant impact on its stress distribution and resonant frequency. Specifically, as the opening angle of the resonant tube increases, the resonant frequency slowly increases, while an increase in the tail cavity radius leads to a rapid decrease in the resonant frequency. In addition, the mutant resonant tube exhibits significant advantages in equivalent stress distribution with its maximum equivalent stress being 31.7% lower than that of the gradual resonant tube.

In modal analysis, this article found that the third mode of the resonant tube is a radial variation, which meets the working requirements of the thermoacoustic refrigeration machine, while the first, the second, the fourth and the fifth modes are shaking variations. By adjusting the opening angle and tail cavity radius of the resonant tube, this paper successfully designed a resonant tube with a resonant frequency close to 2000Hz. This resonant tube can achieve resonance with the acoustic driving frequency under low equivalent stress conditions, output the maximum sound pressure, and thus improve the working efficiency of the thermoacoustic refrigeration machine.

This study provides a universal method for the design of resonant tubes in thermoacoustic refrigerators. By optimizing geometric structural parameters, resonant tube design for specific resonant frequencies can be achieved. This article not only helps to improve the performance of thermoacoustic refrigerators, but also provides theoretical basis and technical support for the design of resonant tubes in practical engineering applications. Future research can further explore the influence of other geometric parameters on the performance of resonant tubes to optimize the design scheme of resonant tubes and promote the development of thermoacoustic refrigeration technology.

References

[1] Yu Y, Zhou J, He W. Effect of tube dimensions on resonant frequency of stepped acoustic resonator [J]. Transactions of the Institute of Measurement and Control, 2024: 01423312241284667.

[2] Chi J, Xu J, Zhang L, et al. Numerical simulation study of gas-liquid coupled double-acting traveling-wave thermoacoustic refrigeration system[J]. Journal of Refrigeration, 2021, 42 (04): 50 - 56.

[3] Hu A, Zhang G, Li C, et al. Resonant frequency of sound wave in a resonance tube with partially closed end [J]. Physics and Engineering, 2023, 33 (01): 115 - 119.

[4] Bouman, Troy M. Development of the Carbon Nanotube Thermoacoustic Loudspeaker [D]. ProQuest Dissertations and Theses Full-text Search Platform, 2021.

[5] Sun W, Chen G, Tang L, et al. Numerical study on acoustic matching between driver and resonator of loudspeaker-driven thermoacoustic refrigerator [J]. International Journal of Green Energy, 2025, 22 (6): 1072 - 1086.

[6] Guo FH, Du JT, Liu Y. Dynamic behavior modeling and energy conversion characteristic analysis of a thermoacoustic-piezoelectric generator with the consideration of thermal and viscous losses [J]. Journal of Sound and Vibration, 2024, 577 118338-.

[7] Gong J. Study on the nonlinear acoustic field of exponential shaped thermoacoustic resonator [D]. Hunan University of Science and Technology, 2016.

[8] Elgezzar M, Rashad A, Hassan M S, et al. CFD simulation with analytical verification of discharging of nitrogen and helium from a high-pressure gas vessel [J]. Journal of Physics: Conference Series, 2023, 2616 (1).

[9] Rezaeepazhand, Amirreza. Modeling and Simulations of 2D Nano-Mechanical Resonators [D]. ProQuest Dissertations and Theses Full-text Search Platform, 2024.

[10] Guo F. Fundamental study on high-frequency miniature standing-wave thermoacoustic refrigerators [D]. Inner Mongolia University of Science and Technology, 2015.